Published OnlineFirst November 17, 2006; DOI: 10.1158/0008-5472.CAN-06-1278

Research Article

Macrophages Regulate the Angiogenic Switch in a Mouse Model of Breast Cancer

Elaine Y. Lin,[1] Jiu-Feng Li,[1] Leoid Gnatovskiy,[1] Yan Deng,[2] Liyin Zhu,[1] Dustin A. Grzesik,[2] Hong Qian,[3] Xiao-nan Xue,[3] and Jeffrey W. Pollard[1]

[1]Department of Developmental and Molecular Biology, Center of Reproductive Biology and Women's Health, [2]Analytical Imaging Facility, and [3]Department of Epidemiology and Population Health, Albert Einstein Cancer Center, Albert Einstein College of Medicine, Bronx, New York

Abstract

The development of a tumor vasculature or access to the host vasculature is a crucial step for the survival and metastasis of malignant tumors. Although therapeutic strategies attempting to inhibit this step during tumor development are being developed, the biological regulation of this process is still largely unknown. Using a transgenic mouse susceptible to mammary cancer, PyMT mice, we have characterized the development of the vasculature in mammary tumors during their progression to malignancy. We show that the onset of the angiogenic switch, identified as the formation of a high-density vessel network, is closely associated with the transition to malignancy. More importantly, both the angiogenic switch and the progression to malignancy are regulated by infiltrated macrophages in the primary mammary tumors. Inhibition of the macrophage infiltration into the tumor delayed the angiogenic switch and malignant transition whereas genetic restoration of the macrophage population specifically in these tumors rescued the vessel phenotype. Furthermore, premature induction of macrophage infiltration into premalignant lesions promoted an early onset of the angiogenic switch independent of tumor progression. Taken together, this study shows that tumor-associated macrophages play a key role in promoting tumor angiogenesis, an essential step in the tumor progression to malignancy. (Cancer Res 2006; 66(23): 11238-46)

Introduction

Tumor progression is characterized by an initial "avascular phase" when the tumors are small and usually dormant (1) with diffusion being the major way to support their metabolic needs (2). In the subsequent "vascular phase," the development of a unique tumor vasculature is required for the increased metabolic demand of tumors that have grown beyond a certain size. The induction of this vasculature, termed the "angiogenic switch" (1, 3, 4), can occur at various stages of tumor progression, depending on the tumor type and the environment (1). However, it is clear that malignant tumors require its development as it has been shown that the initiation of revascularization in dormant lesions allows them to progress (5, 6).

The stroma of solid tumors are replete with many leukocytic cells of which macrophages represent a major component (7). Recent clinical and experimental studies have indicated that these tumor-associated macrophages promote the progression to malignancy (7, 8). In human breast cancers, macrophages cluster in "hotspots" in avascular areas in human breast cancer samples (9), which correlates with a high level of angiogenesis and with decreased relapse-free and overall survival of the patients (10). Macrophages play a crucial role in regulating angiogenesis in wound healing (11). They produce many proangiogenic factors including vascular endothelial growth factor (VEGF), tumor necrosis factor α, granulocyte macrophage colony-stimulating factor, interleukin (IL)-1, IL-6 (11), and other factors including matrix metalloproteinases (MMP) and nitric oxide (12, 13) that also have the potential to regulate angiogenesis (7, 11). Parallels have been drawn between the microenvironment of wound-induced inflammation and that of tumors, as proposed in the hypothesis that tumors are "wounds that never heal" (14). However, whether tumor-associated macrophages are able to promote angiogenesis is still not clear.

We have reported in the mouse model of breast cancer caused by the mammary epithelial cell restricted expression of the Polyoma middle T oncoprotein (PyMT mice) that the infiltration of macrophages in primary mammary tumors was positively associated with tumor progression to malignancy (8). Depletion of macrophages in this model severely delayed tumor progression and dramatically reduced metastasis whereas an increase in macrophage infiltration by transgenic means remarkably accelerated these processes (8). To identify the mechanism(s) that macrophages use to promote tumor progression, we have tested the hypothesis that tumor-associated macrophages stimulate the development of tumor vasculature. Our results indicate that tumor-associated macrophages were actively involved in promoting the angiogenic switch during the malignant transition as well as in the maintenance and/or remodeling of an established vessel network in malignant tumors.

Materials and Methods

Mice. All procedures involving mice were conducted in accordance with NIH regulations about the use and care of experimental animals. The study of mice was approved by the Albert Einstein College of Medicine animal use committee. The PyMT transgenic mice and mice carrying the CSF-1R-GFP transgene were kindly provided by Drs. W.J. Muller (McGill University, Montreal, Quebec, Canada) and David Hume (University of Brisbane, Brisbane, Australia), respectively. The origin, care, and identification of CSF-1 null mutant ($Csf1^{op}/Csf1^{op}$) mice have previously been described (8). Because $+/Csf1^{op}$ mice have normal serum concentration of CSF-1, normal tissue population of macrophages, and are in all aspects tested equivalent to wild-type (+/+) mice (15), these $+/Csf1^{op}$ are used as controls. The preparation of CSF-1-expressing transgenic mice has previously been described (8). The mice used were in a mixed genetic background of C3H/B6/FVB. The genotype of the CSF-1R-GFP mice was determined by directly

Requests for reprints: Jeffrey W. Pollard, Albert Einstein College of Medicine, 607 Chanin Building, 1300 Morris Park Avenue, Bronx, NY 10461. Phone: 718-430-2090; Fax: 718-430-8663; E-mail: pollard@aecom.yu.edu.

doi:10.1158/0008-5472.CAN-06-1278

Published OnlineFirst November 17, 2006; DOI: 10.1158/0008-5472.CAN-06-1278

visualizing the green fluorescent protein (GFP) expression in blood monocytes.

***In vivo* vessel labeling methods.** Texas red–conjugated dextran (mol wt 70,000; Molecular Probes, Eugene, OR) was prepared to 6.2 mg/mL in PBS; 21 μg/g of mouse body weight was i.v. injected. The mice were killed for tissue preparation 5 minutes after the injection. For the *Lycopersicon esculentum* lectin (LEL)/dextran colabeling, 1.3 μg FITC-conjugated LEL (Sigma)/g body weight were mixed with dextran solution in the concentration described above and injected into the tail vein. For analysis, tumors were isolated and fixed with formalin, paraffin embedded, and sectioned following standard procedures.

Macrophage labeling and quantitative analysis. Immunohistochemistry of macrophage with rat anti-mouse F4/80 antibody was previously described (8). To measure the macrophage density in tumors, immunohistochemically stained sections were photographed to TIFF Images using an Olympus IX70 microscope and a Sensicam QE cooled CCD camera. Macrophages in the vicinity of a lesion were measured and normalized by the circumference of the lesion using ImageJ program. To prepare tissue sections from CSF-1R-GFP transgenic mice, tissues were fixed in 5% formalin in 20% sucrose/PBS solution at 4°C for 24 hours followed by freezing and sectioning. To label macrophages using dextran, 21 μg/g mouse body weight of FITC-conjugated dextran (Molecular Probes) were i.v. injected and tumors were isolated 1 hour after the injection. Using transgenic mice expressing GFP specifically in macrophages (CSF-1R-GFP mice), we have observed that within the tumors, only macrophages took up the injected dextran (data not shown). The standard procedure was used for immunohistochemistry of anti-VEGF antibody (Santa Cruz Biotechnology, Santa Cruz, CA) and anti–von Willebrand factor (vWF) antibody (DAKO, Glostrup, Denmark).

Histologic analysis and vessel density measurements. For quantitative analysis of vessel distribution in the tumor, the entire midline section from a lesion was photographed into TIFF images and the area in the lesion marked by dextran was measured using the ImageJ program. For the comparison of vessel density at different stages of progression classified as previously described (16), such dextran-marked areas were normalized by the number of slides for each section and the mean vessel density at different stages was compared. As previously described (8), a large percentage of PyMT mice analyzed at 5 to 6, 7 to 8, 9 to 10, or >12 weeks of age carry mammary lesions at hyperplasia, adenoma/mammary intraepithelial neoplasia (MIN), early carcinoma (EC), and late carcinoma (LC) stages, respectively. To determine the density of the vessels in tumors (Fig. 5*B, iii*), the dextran-marked vasculature was skeletonized using ImageJ program. At least four mice per group were analyzed.

Results

Increased vessel density is associated with the transition to malignancy. Mammary lesions in PyMT mice progress through four stages from a benign hyperplasia to an adenoma/MIN and then to the malignant EC and LC stages (Fig. 1*A*; ref. 8). A high frequency of pulmonary metastasis was detected when the primary mammary tumors progressed to the malignant stages (8, 17). This stereotypic passage through defined stages provides an excellent model to study the relationship of the development of the vasculature according to stage and to test the hypothesis that tumor-associated macrophages play a key role in angiogenesis.

To characterize the development of the vessels in tumors, PyMT mice were i.v. injected with Texas red–conjugated, lysine-fixable dextran 5 minutes before killing. The conjugation of the dextran with lysine allows cross-linking of the florescent dye–labeled dextran onto the vessel wall during fixation to permanently mark the vessels during histologic analysis. This i.v. injection method gives an accurate and quantitative measurement of vessel density and architecture in tumors. It also allows to label functional blood vessels in the tumor (18).

In the passage from hyperplasia to the adenoma/MIN stage (Fig. 1*A*), the tumor mass was obviously increased. However, the density of dextran-marked vessels remained constant (Fig. 1*B, H* versus *A/M*; $P = 0.259$) and was comparable to the density of the vessels surrounded the normal ducts (Fig. 1*B, duct*).

A dramatic change in vessel distribution and density was observed during the transition from the premalignant to the EC malignant stage (Fig. 1*A*; ref. 16). The characteristic feature of the EC-stage lesion is that in the center of the lesion, the acina-like structure is replaced by a small solid nodule in which tumor cells have an increased nuclear pleomorphism and cytologic atypia. The lesion was classified as the transition stage of malignancy because such solid nodule(s) with malignant features were only observed in limited region(s) of the lesion (Fig. 1*A, EC, inset*), whereas the majority of the acini were still at the premalignant stages (Fig. 1*A, EC, arrows*). The high-density vessel network was only found in the solid nodular area (Fig. 1*A, EC*) and not in the surrounding premalignant acini, in which the vessel density was similar to that found in lesions at the premalignant stages (Fig. 1*A, H* and *A/M*). Consistent with these histologic observations, a quantitative analysis indicated a significant increase of vessel density in the solid nodule compared with the lesions at adenoma/MIN stage (Fig. 1*B, A/M* versus *EC*; $P = 0.006$). These observations suggest that such an increase of vessel density is closely associated with the malignant transition in the tumor.

Further changes in vessel distribution and density were observed in primary tumors as they progressed to the most advanced malignant LC stage. A LC-stage lesion consists of multiple large solid nodules that contain layers of tumor cells with little or no remaining acina structure and stroma (Fig. 1*A, LC*). These solid nodules had both high- and low-density vessel networks but the overall density of the vessels was similar to that of the EC-stage lesions (Fig. 1*B, EC* versus *LC*).

To confirm that the dextran injection method could precisely mark blood vessels in tumors, we did a coinjection experiment with the Texas red–conjugated dextran and FITC-conjugated LEL, which specifically binds to endothelial cells (19). Using confocal microscopy, we observed that the majority of dextran-marked channels in the tumors were colocalized with FITC-LEL staining (Fig. 2*A* and *B*). The representative image showed a FITC-LEL–labeled vessel (Fig. 2*B, b*) in the tumor that completely overlapped with the dextran-marked channel (Fig. 2*B, c* and *d*) and the lumen of the channel was filled with RBC (Fig. 2*B, arrows*). There were also some diffuse areas of dextran labeling in cysts or necrotic areas in large tumors (Fig. 2*A, a* and *c, arrows*), suggesting dextran leakage in these areas. These areas of low density and dull staining were not included in our analysis of the vessel density.

The validity of the dextran labeling was further confirmed by immunohistochemistry of tumor sections using antibodies recognizing the endothelial cell–specific marker vWF. As shown in Fig. 2*C*, the pattern of vWF staining (Fig. 2*C, a*) largely overlapped with the dextran labeling in the tumor section (Fig. 2*C, b* and *c*), indicating that dextran-marked channels are lined by vWF-expressing endothelial cells. In fact, there are more vWF-positive areas than dextran-labeled regions in the tumor section (Fig. 2*C, c, arrows*), suggesting that injected dextran only labeled vessels with open lumens or functional blood vessels (18). Higher magnification confirmed that the fluorescently labeled dextran was in the lumen formed by vWF-positive cells (Fig. 2*C, d, arrow*). In addition to the tissue staining, we have also observed the flow of the RBC through all of the dextran-filled channels in tumors of living PyMT mice

Published OnlineFirst November 17, 2006; DOI: 10.1158/0008-5472.CAN-06-1278

using multiphoton microscopy (ref. 20; data not shown). This indicates that all these marked vessels are part of the circulatory system. We can therefore conclude that the dextran injection marked the great majority, if not all, of the active vessels in tumors.

Macrophage infiltration precedes angiogenesis and vascular remodeling in tumors. As a first step in testing the hypothesis that macrophages play a causal role in angiogenesis, we examined the distribution of macrophages at different stages of tumor progression. Few macrophages were found in the hyperplasia and adenoma/MIN tumors in mice between 4 and 6 weeks of age, as determined by immunohistochemistry with antibodies to the macrophage-specific marker F4/80 (Fig. 3*A, white arrows*). In fact, the density of macrophages in these premalignant lesions was similar to that found in the adjacent normal adipose-rich stroma but was significantly lower than macrophages surrounding the developing terminal end buds of normal ducts (data not

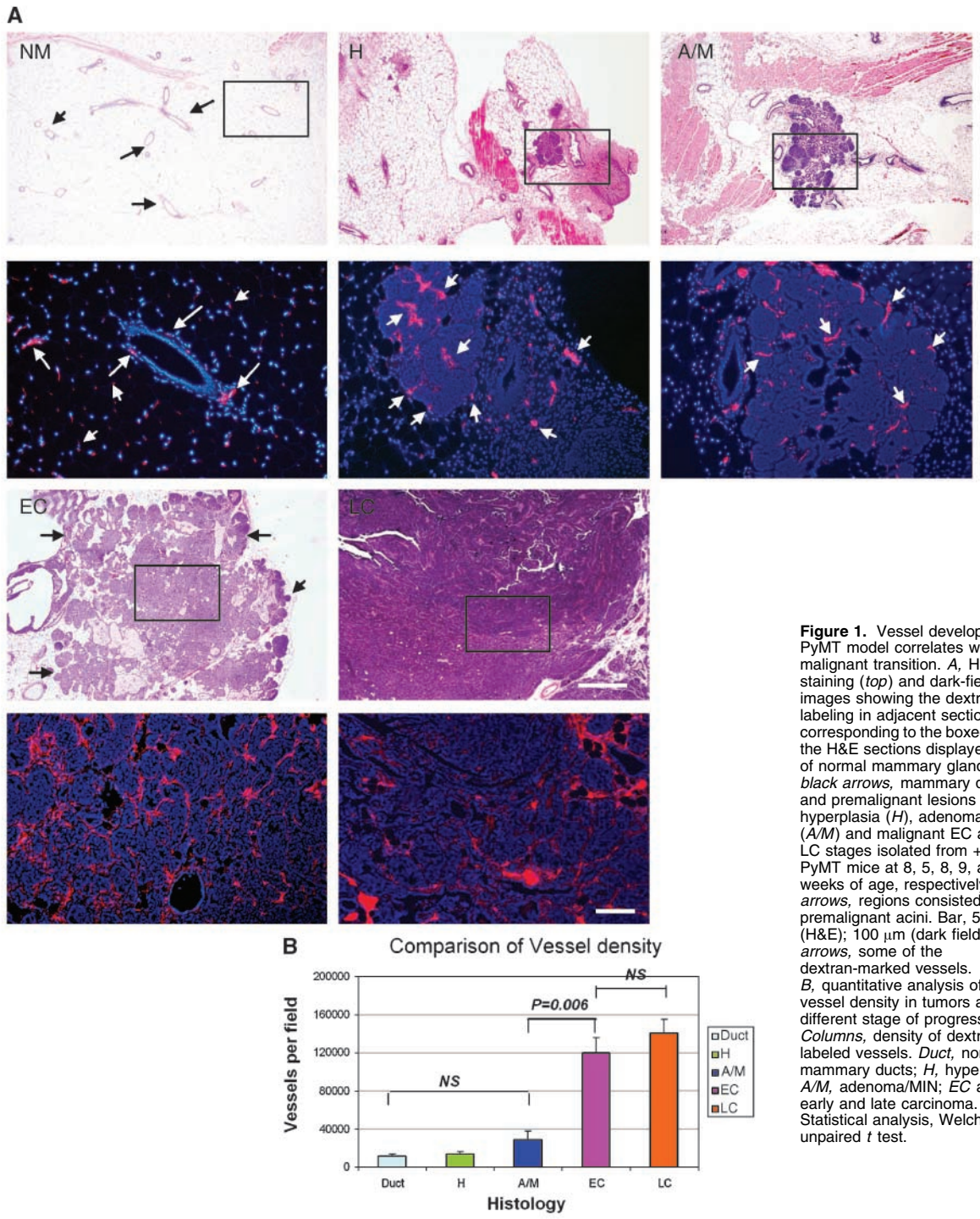

Figure 1. Vessel development in PyMT model correlates with the malignant transition. *A,* H&E staining (*top*) and dark-field images showing the dextran labeling in adjacent sections corresponding to the boxed area in the H&E sections displayed above of normal mammary gland (*NM*; *black arrows,* mammary ducts) and premalignant lesions at hyperplasia (*H*), adenoma/MIN (*A/M*) and malignant EC and LC stages isolated from +/*Csf1*^{op} PyMT mice at 8, 5, 8, 9, and 16 weeks of age, respectively. *EC, arrows,* regions consisted of premalignant acini. Bar, 500 μm (H&E); 100 μm (dark field). *White arrows,* some of the dextran-marked vessels. *B,* quantitative analysis of the vessel density in tumors at different stage of progression. *Columns,* density of dextran-labeled vessels. *Duct,* normal mammary ducts; *H,* hyperplasia; *A/M,* adenoma/MIN; *EC* and *LC*, early and late carcinoma. Statistical analysis, Welch's unpaired *t* test.

Published OnlineFirst November 17, 2006; DOI: 10.1158/0008-5472.CAN-06-1278

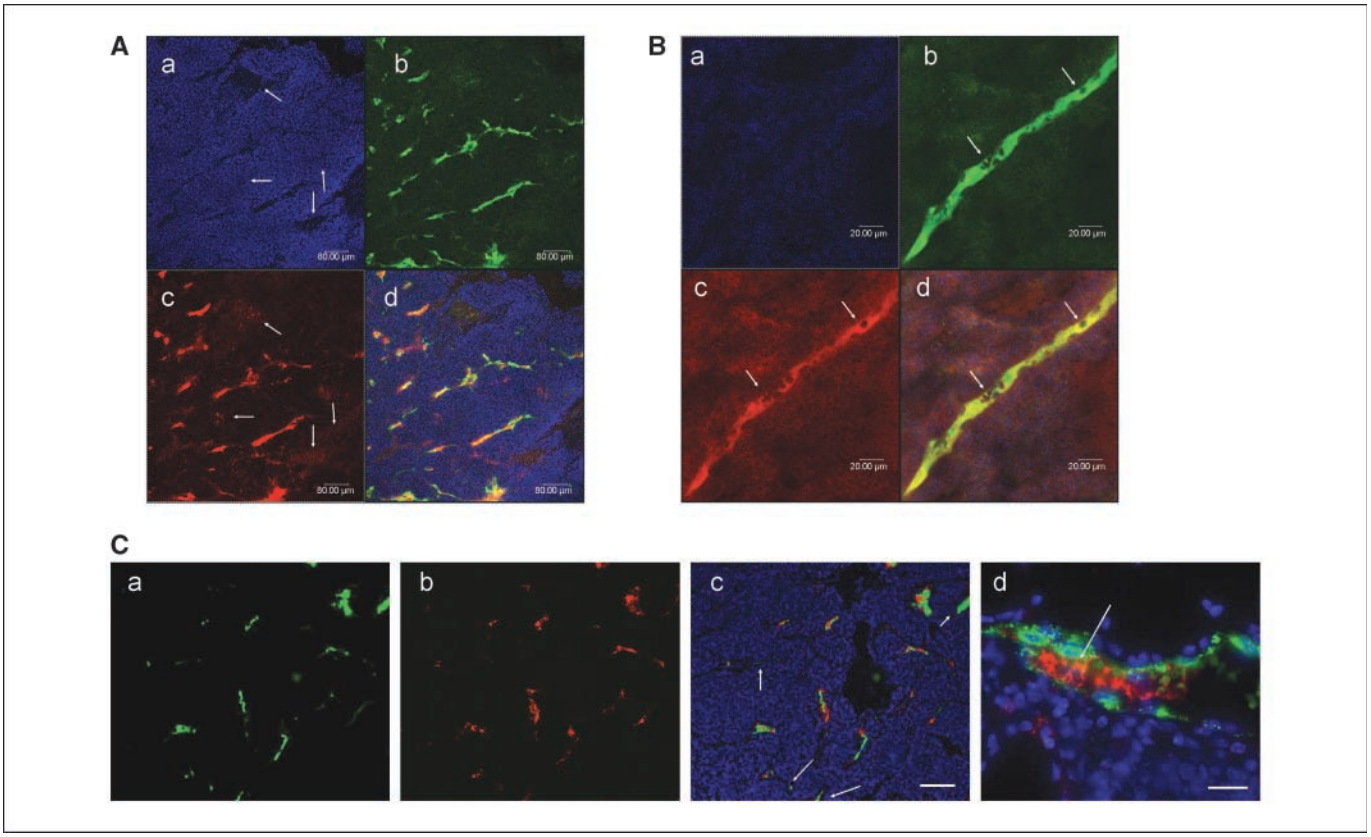

Figure 2. Dextran-marked channels are lined by endothelial cells. *A* and *B,* confocal images of tumor sections from Texas red-dextran and FITC-LEL coinjected PyMT mice at 18 weeks of age. *a,* 4′,6-diamidino-2-phenylindole (DAPI) counterstaining; *b,* FITC-LEL; *c,* Texas red-dextran; *d,* merged image. *A, arrows,* cysts and necrotic areas in the tumor. *B,* blow-up of a vessel in *A. Arrows,* RBC in the lumen of the dextran- or LEL-labeled vessel. Bar, 80 μm (*A*); 20 μm (*B*). *C,* images of tumor sections from a Texas red-dextran–injected PyMT mouse at 16 weeks of age stained with anti-vWF antibody. *a,* vWF staining; *b,* dextran labeling; *c,* overlaid image of *a, b*, and DAPI. *c, arrows,* vessels that are positively stained by vWF antibody but are dextran negative. *d,* a higher magnification image of the staining. *Arrow,* a dextran-filled vessel lumen formed by vWF-positive cells (*green*). Bar, 100 μm (*a-c*); 20 μm (*d*).

shown; ref. 21). However, a remarkable increase in macrophage infiltration occurred in a large percentage of the adenoma/MIN tumors at 7 to 8 weeks of age. Macrophages in these more advanced lesions formed dense clusters in the stroma surrounding the enlarged tumor acini (Fig. 3*A, A/M, right, white arrows*). This infiltration preceded the formation of the dense vessel network.

A large percentage of primary tumors examined at 9 to 10 weeks of age have progressed to the EC stage. These tumors had a further increase in macrophage infiltration. Clusters of high-density infiltrates were found in the vicinity of tumor acini that still were at the adenoma/MIN stage (Fig. 3*B, EC left, white arrows*). These macrophages normally had a rounded morphology. The distribution of the vessels in these areas was also similar to that found in adenoma/MIN lesion (Fig. 3*A*). In contrast, fewer macrophages were found in the center of the tumor where the dense vessel network had developed. In these areas, macrophages were attached to the vessel network and were stretched out along the vessels (Fig. 3*B, EC right, arrows*). Thus, both the morphology and distribution of macrophages were altered depending on the tumor stage and context.

A further increase of macrophage infiltration was observed as tumors progressed to the LC stage. A high density of macrophages was found in a stroma-rich ring surrounding the solid tumor nodules with the characteristics of LC (Fig. 3*B, LC*). In this ring, which also contained a high-density vessel network, a large percentage of macrophages seemed to stretch out and attach to the vessels (Fig. 3*B, LC, arrows*). Similar to the EC, high-density clusters of macrophages were also found in the areas that were still at the adenoma/MIN stage with a corresponding low density of vessels (data not shown).

To confirm the observations of F4/80 staining in tumors, LC-stage lesions from CSF-1R-GFP.PyMT mice were used because the CSF-1R promoter is specifically expressed in macrophages (22). Consistent with the F4/80 staining, a high density of GFP-positive stromal cells was found at the vicinity of the lesion (Fig. 3*C*) and, as seen from the higher power image in the area containing the vessel network, GFP-positive cells were physically associated with the vessel (Fig. 3*C*).

Macrophage depletion inhibits the angiogenic switch and the malignant transition. The data above show a remarkable increase in macrophage infiltration into the nonmalignant primary tumors followed by the formation of a vessel network and the transition to malignancy. This suggests that macrophages may promote these two processes. We next tested whether macrophages play a causal role in angiogenesis by depleting macrophages in tumors using mice carrying the homozygous null allele ($Csf1^{op}$) for the mononuclear phagocyte growth factor CSF-1.

In these studies, we observed a correlation between a low density of macrophages in the primary tumors of CSF-1 null mutant mice

Published OnlineFirst November 17, 2006; DOI: 10.1158/0008-5472.CAN-06-1278

and a marked delay in the angiogenic switch that was associated with a significant delay in the malignant transition (8). In contrast to the tumors in heterozygous controls, in which the formation of dense vessel networks was found in the mammary lesions as early as 8 weeks of age (Fig. 4*A, a*), a large percentage of CSF-1 null mutant mice did not develop such networks in their primary tumors even when they reached 18 weeks of age (Fig. 4*A, b*). This was the case even though most of these lesions were larger than 8 mm^3 in size. In addition, a "sponge" like structure was often seen in these CSF-1 null tumors, indicating that these lesions were formed mainly by densely packed hyperplastic duct-like structure instead of the solid nodules that are the characteristic component of malignant lesions (Fig. 4*A, b*).

We next compared tumor progression and angiogenesis in the CSF-1 null mutant mice to their heterozygous littermates at 8 to 9 weeks of age in which ~60% of the +/$Csf1^{op}$ PyMT mice have developed malignant stage tumors. As we have previously observed, a lower percentage of CSF-1 null tumors had progressed to the malignant stages compared with the +/$Csf1^{op}$ controls at the same age (36% versus 60%). Notably, in both genotypes, only those tumors that had progressed to malignant stages developed a vessel network, although still different between genotypes (see below). However, as previously reported (8, 23), despite the complete lack of CSF-1, tumors in mice homozygous for the $Csf1^{op}$ mutation are not completely depleted of macrophages. Thus, we hypothesized that the reason that CSF-1 null mutant mice examined had tumors that had progressed to malignancy at this age was due to the partial recovery of the macrophage population in these tumors.

To test this, we compared the macrophage density in tumors that either progressed or failed to progress to malignancy at this age. A quantitative analysis was done by measuring the density of macrophages in the surrounding stroma relative to the circumference of the tumor section. As commented on above but now presented numerically, in +/$Csf1^{op}$ tumors, a significantly higher density of macrophages was found in tumors as they progressed from the hyperplastic to adenoma to the malignant stages (Fig. 4*B, Pre, 6w* versus *9w*). This resulted in an almost 50-fold increase in macrophage density in malignant tumors compared with the hyperplastic ones. Although the macrophage density in CSF-1 null

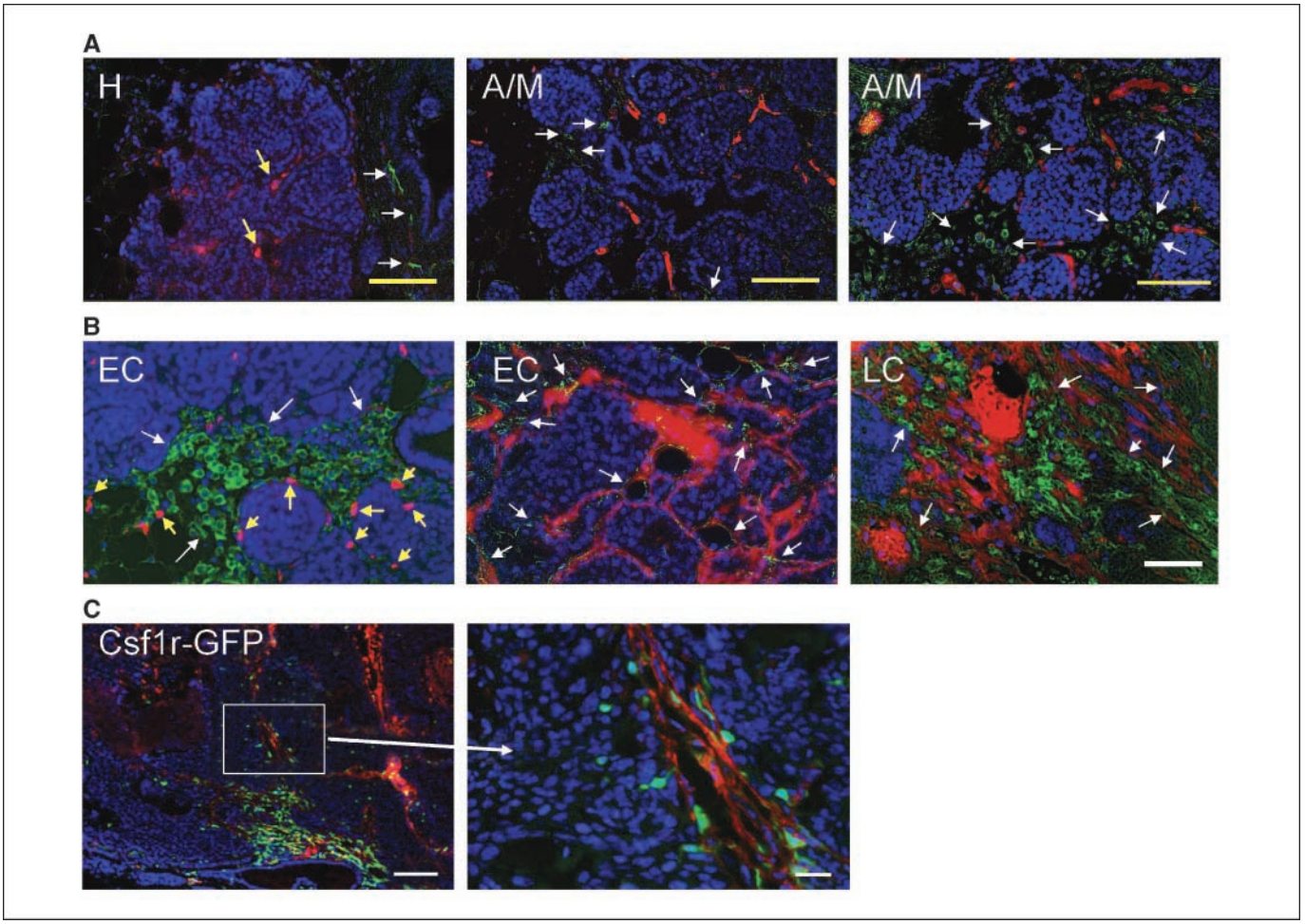

Figure 3. Macrophage infiltration in primary mammary tumors correlates with vessel network development and tumor progression. Immunohistochemistry using anti-F4/80 antibodies of tumor sections stained with DAPI from Texas red-dextran–injected +/Csf^{op} PyMT mice. The staining from immunohistochemistry was converted to green using Photoshop. Tumors were isolated from +/$Csf1^{op}$ PyMT mice at 5 weeks (*H*), 6 weeks (*A/M, left*), 9 weeks (*A/M, right*), 9 weeks (*EC*), and 17 weeks (*LC*) of age, respectively. *A,* lesions are at the hyperplasia (*H*) and adenoma/MIN (*A/M*). Yellow size bars in H and A/M sections, 100 μm. *B,* lesions are at EC and LC stages. *White arrows,* some of the F4/80+ macrophages; *yellow arrows,* dextran-labeled vessels. White size bar in EC and LC sections, 50 μm. *C,* LC-stage tumor sections from a Texas red-dextran–injected CSF1R-GFP transgenic mouse. The inset on the left (bar, 100 μm) is shown at higher magnification on the right (bar, 20 μm). *Arrows,* GFP-positive macrophages.

Published OnlineFirst November 17, 2006; DOI: 10.1158/0008-5472.CAN-06-1278

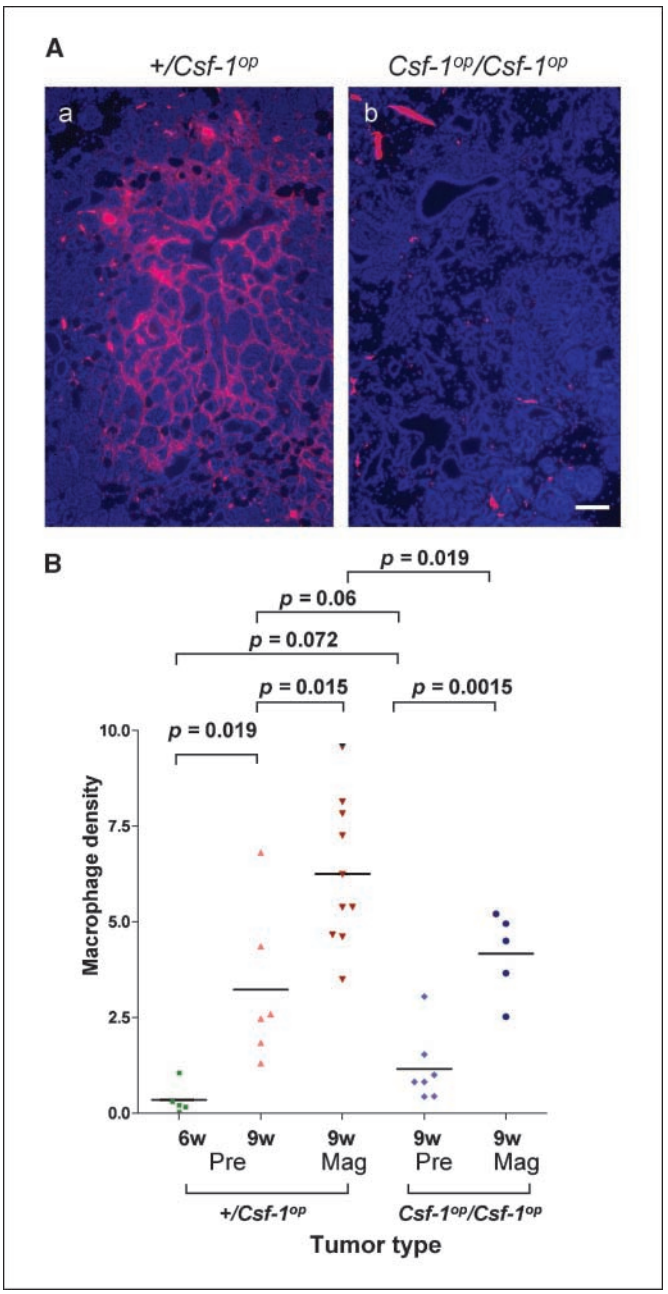

Figure 4. The relationship between macrophage infiltration and malignant transition. *A,* delayed angiogenic switch and malignant transition in macrophage depleted tumors. Tumor sections from a +/*Csf1*^{op} mouse at 8 weeks of age (*a*) and from a *Csf1*^{op}/*Csf1*^{op} mouse at 18 weeks of age (*b*) injected with Texas red–conjugated dextran. The tumor sections were stained with DAPI. Bar, 100 μm. *B,* a quantitative analysis of macrophage density in +/*Csf1*^{op} and CSF-1 null tumors, *Csf1*^{op}/*Csf1*^{op}. *6w* or *9w,* mice were at 5 to 6 or 8 to 9 weeks of age, respectively. *Pre,* tumors were at premalignant stages; *Mag,* tumors were at malignant stages. The data were prepared as described in Materials and Methods and analyzed using Welch's unpaired *t* test.

tumors at the premalignant stage was ~25% of that found in the +/*Csf1*^{op} lesions at the same stage, this only bordered on significance probably because of the wide variation in wild-type mice as they were dynamically transitioning into the malignant state (Fig. 4*B*). This similarity in density is consistent with the similar rates of progression and growth rates of these premalignant tumors in both genotypes. However, a significantly higher level of macrophage density was also found in the CSF-1 null tumors as they progressed to the malignant stages compared with the CSF-1 null tumors at the premalignant stages (Fig. 4*B*). This positive correlation of macrophage density and tumor progression to malignancy in both genotypes argues that tumor-associated macrophages have a direct effect on the malignant transition and the angiogenic switch because this is always associated with the malignant transition. Nevertheless, when comparing the macrophage density in CSF-1 null tumors to that in +/*Csf1*^{op} tumors at the malignant stages, there was a significantly lower density of macrophages in CSF-1 null tumors at the same stage (Fig. 4*B*). This result indicates that a relatively low density of macrophage in these CSF-1 null tumors is sufficient for the malignant transition and angiogenic switch but that it might be the cause of a slower rate of progression and inhibition of metastasis as previously observed (8).

As shown above, even in malignant tumors, the CSF-1 null mice had lower numbers of macrophages. Thus, we tested whether such a low density had any effect on the development of tumor vasculature in tumors that had progressed to late-stage malignancy in age-matched mice. This selection of equivalently matched tumors prevented bias that could be caused by comparing tumors at different stages of progression. We found that, despite the formation of a vessel network in the CSF-1 null tumors (Fig. 5*A,* −/−), a much lower density of such networks was observed in these lesions compared with their +/*Csf1*^{op} counterparts (Fig. 5*A,* +/−). This was directly due to the absence of macrophages in the tumors because restoration of macrophage numbers in the tumors of *Csf1*^{op}/*Csf1*^{op} mice by the transgenic expression of CSF-1 specifically in the mammary epithelium (8) resulted in the vessel density returning to the +/*Csf1*^{op} level (Fig. 5*A, Trans*).

To confirm these histologic observations, a quantitative analysis of the tumor was done to compare vessel area and density. Sections of the entire LC-stage tumors of all three genotypes were imaged and the area covered with vessels in each section was highlighted and the total area occupied per section was measured as described in Materials and Methods (Fig. 5*B, ii*). Afterwards, the images were skeletonized to analyze the vessel density (Fig. 5*B, iii*). This method allows vessels with either big or small lumens to be represented as lines with similar thickness (pointed by blue or red arrows, respectively) such that total vessel length could be measured (Fig. 5*B, arrows*).

Based on the analysis of more than 300 images, the mean areas in LC-stage tumors covered by the vessels was 40% lower in CSF-1 null tumors compared with their +/*Csf1*^{op} counterparts (Fig. 5*C, OP* versus *WT*; $P = 0.014$). Similarly, the vessel density in CSF-1 null LC-stage tumors was significantly lower than +/*Csf1*^{op} controls (Fig. 5*D, OP* versus *WT*; $P = 0.03$). Restoration of the infiltration of macrophages by expression of CSF-1 in the CSF1 null tumors increased this vessel area to a level similar to the +/*Csf1*^{op} tumors (Fig. 5*C, WT* versus *TRANS*; $P = 0.35$) and also restored the vessel density to the +/*Csf1*^{op} level (Fig. 5*D, WT* versus *TRANS*; $P = 0.29$). A similar difference (~1.8-fold) was found when comparing the areas covered by vessels and vessel densities between +/*Csf1*^{op} and CSF-1 null tumors, suggesting that the sizes of the vessel lumens in these two genotypes were similar. Taken together, these data indicated that the infiltration of macrophages in tumors regulates the density of vessels in LC-stage tumors with a high level of macrophage infiltration correlated with a high density of vessels.

Published OnlineFirst November 17, 2006; DOI: 10.1158/0008-5472.CAN-06-1278

Premature macrophage infiltration enhances angiogenesis. The results presented above suggest that macrophages induce both the formation of the dense vessel network and the malignant transition. However, based only on these data, it was difficult to determine whether the vasculature development during the malignant transition was directly regulated by macrophages or whether it was a secondary effect induced by this malignant transition consequent to other effects of macrophages. To distinguish between these possibilities, we examined vasculature development in +/*Csf1*^{op} PyMT mice carrying the MMTV LTR-CSF-1 transgene. Because the MMTV LTR in these transgenic PyMT mice is active early in mammary gland development, the expression of the transgenic CSF-1 is induced in young mice independent of tumor progression. We have previously reported that a striking increase in macrophage infiltration was observed in the tumors of these transgenic mice at a young age (8), and that this correlated with accelerated tumor progression and a doubling of the metastatic rate compared with the nontransgenic +/*Csf1*^{op} PyMT mice (8).

In the CSF-1-overexpressing transgenic mice, we found that a dense vessel network developed prematurely in premalignant tumors from mice at 5 weeks of age (Fig. 6*A, top, white arrows*). This dramatic enhancement of the vessel network appeared several weeks earlier than in the nontransgenic controls. Importantly, in the nontransgenic mice, such dense vessel networks were found exclusively in tumors at the malignant stages (Fig. 6*A, +/op-9wk*) whereas in the CSF-1 transgenic mice, the network was already formed in tumors still at premalignant adenoma/MIN (Fig. 6*A, top right*) and even at the earliest premalignant stage, hyperplasia (Fig. 6*A, top left*). No such dense vessel network was ever seen in non-CSF-1 transgenic PyMT mice at the hyperplasia stage (Fig. 6*A, +/op-5wk*). In parallel with the elevated angiogenesis, a high level of macrophage infiltration was observed in the stroma of the CSF-1 transgenic premalignant tumors (Fig. 6*A, top, yellow arrows*) compared with tumors from nontransgenic mice at similar ages (Fig. 6*A, +/op-5wk*) or at the EC stage (Fig. 6*A, +/op-9wk, yellow arrows*). A quantitative analysis of macrophage density in these tumors confirmed a 6-fold increase of macrophage infiltration in the tumors of CSF-1 transgenic +/*Csf1*^{op} PyMT mice compared with the nontransgenic controls (Fig. 6*B*; $P = 0.045$). This observation shows that macrophages have a direct effect on the formation of the vessel network independent of the transition to malignancy, and that the formation of such a network enables tumors to advance to malignancy. A possible mechanism for this is the observation that the major angiogenic regulator, VEGF, was depleted in stromal cells of tumors of CSF-1 null mutant mice

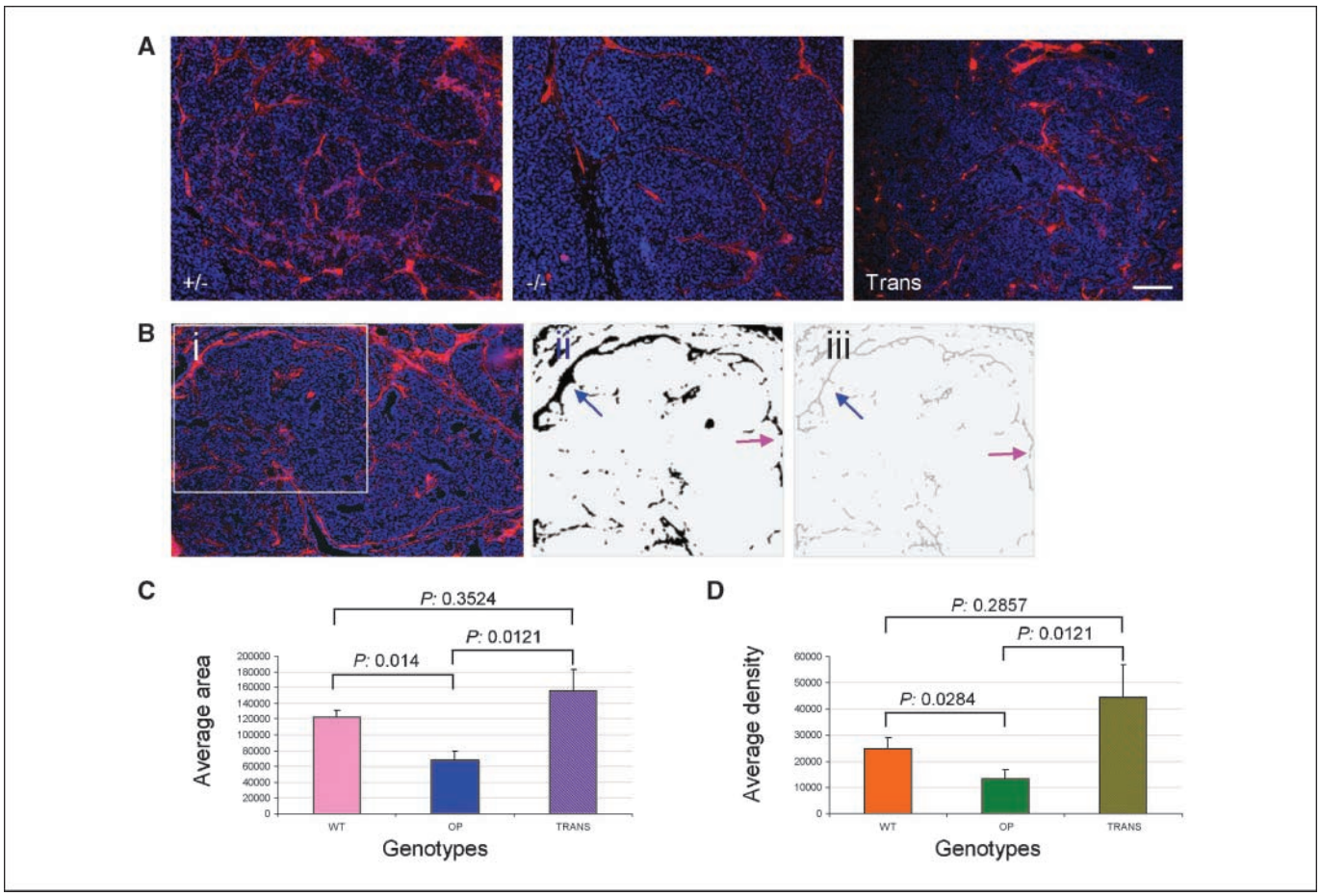

Figure 5. Vessel density in advanced carcinoma correlates with the degree of macrophage infiltration. *A,* vessel distribution in LC-stage tumors from a +/*Csf1*^{op} (+/−), a CSF-1 null (−/−), or a CSF-1 transgenic *Csf1*^{op}/*Csf1*^{op} PyMT mouse (*Trans*) at 16 weeks of age. Bar, 100 μm. *B,* processed images for the vessel density comparison of a tumor section from a Texas red-dextran–injected mouse counterstained with DAPI (*i*). The area marked by dextran was highlighted using ImageJ program and skeletonized to indicate the length of individual vessels (*ii* and *iii*). *Blue arrows,* thick vessels that were represented as thin lines after the image was skeletonized. *Red arrows,* thin vessels in both images. *C,* a comparison of areas in tumors covered by dextran-marked vessels. *D,* comparison of vessel density. *WT,* +/*Csf1*^{op}; *OP,* CSF-1 null or *Csf1*^{op}/*Csf1*^{op}; *TRANS,* CSF-1 transgenic *Csf1*^{op}/*Csf1*^{op} mice. Significance following analysis by the Mann-Whitney test.

Published OnlineFirst November 17, 2006; DOI: 10.1158/0008-5472.CAN-06-1278

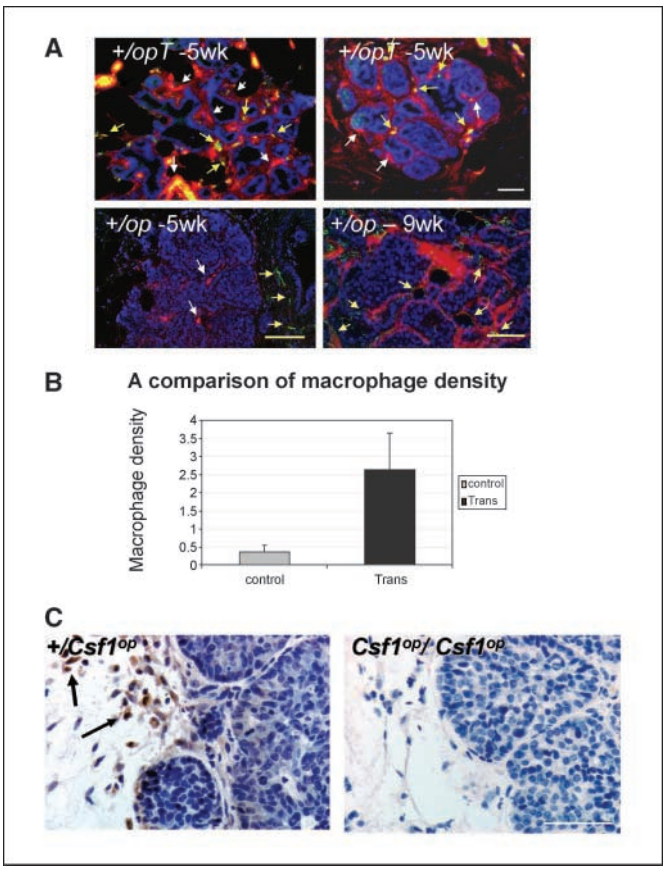

Figure 6. Premature expression of CSF-1 induces vessel network formation in premalignant lesions. *A, +/opT* sections from a hyperplasia (*left*) and adenoma (*right*) from CSF-1 transgenic +/*Csf1*^{op} PyMT mouse at 5 weeks of age. Blood vessels in the tumor were labeled by i.v. injection of Texas red-dextran (*white arrows*) and macrophages were labeled by FITC-conjugated dextran (*yellow arrows*). Bar, 100 μm. *+/op-5wk,* representative image of F4/80 immunohistochemistry of a tumor lesion at hyperplasia stage isolated from a +/*Csf1*^{op} PyMT mouse at 5 weeks of age. Note that the densities of both vessels (*white arrows*) and macrophages (*yellow arrows*) are much lower than in the *+/opT* sections. Bar, 100 μm. *+/op-9wk,* representative F4/80 immunohistochemistry image of a lesion at the EC stage isolated from a +/*Csf1*^{op} PyMT mouse at 9 weeks of age. Note that macrophages (*yellow arrow*) seem to attach to the vessels network. Bar, 50 μm. *B,* quantitative analysis of macrophage infiltration in CSF-1 transgenic (*Trans*) and nontransgenic (*Control*) +/*Csf1*^{op} PyMT mice at 5 to 6 weeks of age. *Columns,* mean; *bars,* SD. *C,* immunohistochemistry for VEGF in LC-stage tumor sections from a +/*Csf1*^{op} or a *Csf1*^{op}/*Csf1*^{op} PyMT mouse at 18 weeks of age. VEGF-positive cells were mainly in stroma as indicated by arrows. Representative of those obtained from six +/*Csf1*^{op} and five *Csf1*^{op}/*Csf1*^{op} PyMT mice with tumors at LC stage.

compared with +/*Csf1*^{op} mice, suggesting that this may be a significant part of the reason for this reduced angiogenesis (Fig. 6*C*). Thus, overexpression of macrophage VEGF may have caused the premature vessel formation.

Discussion

Studies in dormant and malignant tumors have suggested that malignant tumors require the development of a unique vasculature (5, 6). In this article, using a mouse model where the mammary tumors undergo a natural progression through premalignant to malignant stages, we show that the angiogenic switch is required for the malignant transition.

At the malignant transition, although the lesions mostly consist of premalignant acini, small solid nodules form in the center that are the site of the initial malignant transition (16). The angiogenic switch, identified by the formation of a dense vascular network, occurred exclusively in this malignant transition region. This is consistent with other studies using transgenic mouse models of cancers in which a transition stage, termed angiogenic dysplasia, occured before the malignant carcinoma was identified (24–28). However, the close association between the angiogenic switch and malignant transition was not reported in these studies. Furthermore, by manipulating the formation of the vasculature, we were able to show that this angiogenic switch was required for the malignant transition. In support of this conclusion was the delay in the malignant transition following the inhibition of the formation of such vascular networks in CSF-1 null mutant mice. Even more decisive was the accelerated progression of the tumor to malignancy following premature induction of the angiogenic switch in premalignant lesions in the CSF-1 transgenic +/*Csf1*^{op} mice.

Tumors are highly populated with macrophages, and in clinical studies of breast cancer their density correlates with areas of angiogenesis and with poor prognosis (9). Despite these clinical correlations, the role(s) of macrophages in promoting tumor angiogenesis is largely unexplored. In this study, we show that macrophages promote the development of the tumor vasculature. We observed an increase of macrophage infiltration in the stroma of primary tumors shortly before the development of a dense vessel network in the area. Depletion of this macrophage infiltration inhibited the angiogenic switch. Furthermore, increased macrophage infiltration in premalignant lesions through the transgenic expression of CSF-1, of which the only target is CSF-1 receptor–bearing macrophages (8, 29), induced premature formation of the vessel network and accelerated the malignant transition (8). These data indicate that macrophages have a direct effect on angiogenesis and regulate the angiogenic switch.

This study identified a unique feature of tumor vasculature in the PyMT model that reflects the evolution of the tumor through benign to malignant stages. We found that a dense vessel network is initiated in the center of the PyMT lesion only where the malignant transition occurs. This contrasts with that observed in transplanted tumors that are uniform in malignant progression and that need to gain vascular support from the host for the survival of the graft. Therefore the vasculature development that occurs at the periphery of the tumor (30) does not reflect the angiogenic switch in naturally evolving cancers. This is different from PyMT tumors that develop spontaneously and establish a vascular system in premalignant stages that is similar to that observed in the surrounding normal tissues. Therefore, the angiogenic switch identified in this model more closely reflects that seen during human cancer progression.

Our studies here indicated that the angiogenic switch was not simply induced by the expansion of tumor size. We found that the formation of the dense vessel network was initiated in the malignant transition region of EC-stage lesion that was often <1 mm^3 in sizes. This indicates that the event is not induced by the overall growth of the lesion but is stimulated by a regional factor(s) associated with the progression of the tumor cells to malignancy. Furthermore, the angiogenic switch was not detected in more than 40% of CSF-1 null mutant mice that reached 16 weeks of age whereas all of the wild-type mice at this age had tumors developed to the most advanced malignant stage with vessel network formation. Interestingly, although the angiogenic switch was not detected in these CSF-1 null tumors, most of the

Published OnlineFirst November 17, 2006; DOI: 10.1158/0008-5472.CAN-06-1278

tumors were often >8 mm^3, further confirming this lack of association with size.

This study has shown that macrophages play a causal role in promoting tumor angiogenesis and the induction of macrophage infiltration in tumors of PyMT model occurred over a narrow time frame when lesions are still at premalignant stage and small in size. These observations suggest that the tumor microenvironment at the premalignant stage produces local factors that attract the infiltration of macrophages that promote tumor angiogenesis. Studies have shown that tumor cells produce various chemoattractants for leukocytes including CSF-1, CCL2, CCL5, VEGF, and IL-8 (11), suggesting that such infiltration might be manipulated by tumor cells. Clearly, overexpression of CSF-1 is sufficient to recruit abundant macrophages. This is consistent with the clinical observation that overexpression of CSF-1 correlates with leukocytic infiltration, which in turn correlates with poor prognosis (31, 32). This raises the question of what tumor and/or environmental factor(s) triggers the release of these leukocytic chemoattractants. Numerous studies suggest that hypoxia might be the factor that induces the up-regulation of chemoattractants in tumor cells (33). However, we did not see any obvious colocalization of macrophage infiltration and hypoxia in tumors when Hypoxyprobe-1 (pimonidazole hydrochloride) was used to map the hypoxia regions in the PyMT model (data not shown).

The mechanisms macrophages use to promote angiogenesis in tumor are unclear. Macrophages can produce angiogenesis regulators (7, 11) and may also induce tissue remodeling by producing various proteinase activators and inhibitors that may destroy the integrity of the basement membrane and extracellular matrix, liberating matrix-bound factors. Indeed, a recent study using the human papillomavirus-16–induced model of cervical carcinoma showed that macrophages produce MMP-9 that seems to be required for release of VEGF locally in the tumor, and that inhibition of this by bisphosphonate inhibited angiogenesis and reduced tumor incidence and growth (25). Furthermore, inhibition of CSF-1 function in human tumors xenografted into immunocompromized mice reduced their growth and this was correlated with poor macrophage recruitment and reduced angiogenesis due to a depletion of VEGF (34). Indeed, we showed that most of the VEGF-expressing cells in the PyMT model were in stroma and that that they were reduced in the CSF-1 null tumors and presumably, therefore, are macrophages.

In summary, this study uses genetic means to show that macrophages regulate the angiogenic switch, an essential step for the progression of mammary tumors to malignancy. Such information will be very important for the development of novel and effective therapeutic strategies against tumors.

Acknowledgments

Received 4/7/2006; revised 8/2/2006; accepted 9/1/2006.

Grant support: Albert Einstein Cancer Center Analytical Imaging Facility and histopathology facilities, National Cancer Institute grants CA 94173 and CA 100324, and Albert Einstein Cancer Center Core grant P30 CA 13330.

The costs of publication of this article were defrayed in part by the payment of page charges. This article must therefore be hereby marked *advertisement* in accordance with 18 U.S.C. Section 1734 solely to indicate this fact.

We thank Dr. J.E. Segall for critical comments on the manuscript; Drs. S. Patan, A.W. Ashton, R.N. Kitsis, B. Terman, P. Davies, A. Orlofsky, and V. Gouon-Evans for helpful suggestions; and Jim Lee for technical support.

References

1. Bergers G, Benjamin LE. Tumorigenesis and the angiogenic switch. Nat Rev Cancer 2003;3:401–10.
2. Folkman J. How is blood vessel growth regulated in normal and neoplastic tissue? G.H.A. Clowes Memorial Award lecture. Cancer Res 1986;46:467–73.
3. Coussens LM, Tinkle CL, Hanahan D, Werb Z. MMP-9 supplied by bone marrow-derived cells contributes to skin carcinogenesis. Cell 2000;103:481–90.
4. Folkman J. Incipient angiogenesis. J Natl Cancer Inst 2000;92:94–5.
5. Folkman J, Hahnfeldt P, Hlatky L. Cancer: looking outside the genome. Nat Rev Mol Cell Biol 2000;1:76–9.
6. Hanahan D, Folkman J. Patterns and emerging mechanisms of the angiogenic switch during tumorigenesis. Cell 1996;86:353–64.
7. Pollard JW. Tumour-educated macrophages promote tumour progression and metastasis. Nat Rev Cancer 2004;4:71–8.
8. Lin EY, Nguyen AV, Russell RG, Pollard JW. Colony-stimulating factor 1 promotes progression of mammary tumors to malignancy. J Exp Med 2001;193:727–40.
9. Leek RD, Lewis CE, Whitehouse R, Greenall M, Clarke J, Harris AL. Association of macrophage infiltration with angiogenesis and prognosis in invasive breast carcinoma. Cancer Res 1996;56:4625–9.
10. Leek RD, Harris AL. Tumor-associated macrophages in breast cancer. J Mammary Gland Biol Neoplasia 2002;7:177–89.
11. Crowther M, Brown NJ, Bishop ET, Lewis CE. Microenvironmental influence on macrophage regulation of angiogenesis in wounds and malignant tumors. J Leukoc Biol 2001;70:478–90.
12. Lechner M, Lirk P, Rieder J. Inducible nitric oxide synthase (iNOS) in tumor biology: the two sides of the same coin. Semin Cancer Biol 2005;15:277–89.
13. Lijnen HR. Plasmin and matrix metalloproteinases in vascular remodeling. Thromb Haemost 2001;86:324–33.
14. Dvorak HF. Tumors: wounds that do not heal. Similarities between tumor stroma generation and wound healing. N Engl J Med 1986;315:1650–9.
15. Pollard JW, Stanley ER. Pleiotropic roles for CSF-1 in development defined by the mouse mutation osteopetrotic (op). Advances in Developmental Biochemistry 1996;4:153–93.
16. Lin EY, Jones JG, Li P, et al. Progression to malignancy in the polyoma middle T oncoprotein mouse breast cancer model provides a reliable model for human diseases. Am J Pathol 2003;163:2113–26.
17. Guy CT, Cardiff RD, Muller WJ. Induction of mammary tumors by expression of polyomovirus middle T oncogenes: a transgenic mouse mode of a metastatic disease. Mol Cell Biol 1992;12:954–61.
18. McDonald DM, Choyke PL. Imaging of angiogenesis: from microscope to clinic. Nat Med 2003;9:713–25.
19. Ezaki T, Baluk P, Thurston G, La Barbara A, Woo C, McDonald DM. Time course of endothelial cell proliferation and microvascular remodeling in chronic inflammation. Am J Pathol 2001;158:2043–55.
20. Condeelis J, Segall JE. Intravital imaging of cell movement in tumours. Nat Rev Cancer 2003;3:921–30.
21. Gouon-Evans V, Rothenberg ME, Pollard JW. Postnatal mammary gland development requires macrophages and eosinophils. Development 2000;127:2269–82.
22. Sasmono RT, Oceandy D, Pollard JW, et al. A macrophage colony-stimulating factor receptor-green fluorescent protein transgene is expressed throughout the mononuclear phagocyte system of the mouse. Blood 2003;101:1155–63.
23. Cecchini MG, Dominguez MG, Mocci S, et al. Role of colony stimulating factor-1 in the establishment and regulation of tissue macrophages during postnatal development of the mouse. Development 1994;120:1357–72.
24. Calvo A, Yokoyama Y, Smith LE, et al. Inhibition of the mammary carcinoma angiogenic switch in C3(1)/SV40 transgenic mice by a mutated form of human endostatin. Int J Cancer 2002;101:224–34.
25. Giraudo E, Inoue M, Hanahan D. An amino-bisphosphonate targets MMP-9-expressing macrophages and angiogenesis to impair cervical carcinogenesis. J Clin Invest 2004;114:623–33.
26. Parangi S, O'Reilly M, Christofori G, et al. Antiangiogenic therapy of transgenic mice impairs *de novo* tumor growth. Proc Natl Acad Sci U S A 1996;93:2002–7.
27. Bergers G, Javaherian K, Lo KM, Folkman J, Hanahan D. Effects of angiogenesis inhibitors on multistage carcinogenesis in mice. Science 1999;284:808–12.
28. Coussens LM, Raymond WW, Bergers G, et al. Inflammatory mast cells up-regulate angiogenesis during squamous epithelial carcinogenesis. Genes Dev 1999;13:1382–97.
29. Wyckoff J, Wang W, Lin EY, et al. A paracrine loop between tumor cells and macrophages is required for tumor cell migration in mammary tumors. Cancer Res 2004;64:7022–9.
30. Gilead A, Meir G, Neeman M. The role of angiogenesis, vascular maturation, regression and stroma infiltration in dormancy and growth of implanted MLS ovarian carcinoma spheroids. Int J Cancer 2004;108:524–31.
31. Scholl SM, Pallud C, Beuvon F, et al. Anti-colony-stimulating factor-1 antibody staining in primary breast adenocarcinomas correlates with marked inflammatory cell infiltrates and prognosis. J Natl Cancer Inst 1994;86:120–6.
32. Tang RP, Kackinski B, Validire P, et al. Oncogene amplification correlates with dense lymphocyte infiltration in human breast cancers: a role for hematopoietic growth factor release by tumor cells? J Cell Biochem 1990;44:189–98.
33. Murdoch C, Giannoudis A, Lewis CE. Mechanisms regulating the recruitment of macrophages into hypoxic areas of tumors and other ischemic tissues. Blood 2004;104:2224–34.
34. Aharinejad S, Abraham D, Paulus P, et al. Colony-stimulating factor-1 antisense treatment suppresses growth of human tumor xenografts in mice. Cancer Res 2002;62:5317–24.

Cancer Research
The Journal of Cancer Research (1916–1930) | The American Journal of Cancer (1931–1940)

AACR American Association for Cancer Research

Macrophages Regulate the Angiogenic Switch in a Mouse Model of Breast Cancer

Elaine Y. Lin, Jiu-Feng Li, Leoid Gnatovskiy, et al.

Cancer Res 2006;66:11238-11246. Published OnlineFirst November 17, 2006.